Nonlinear Dynamics of Charge Pump Phase-Locked Loops

Raymond Flynn, Paul Curran and Orla Feely

Department of Electronic and Electrical Engineering, University College Dublin,
Belfield, Dublin 4, Ireland.

Email: ray.flynn@ee.ucd.ie, paul.curran@ucd.ie, orla.feely@ucd.ie

Abstract– This paper presents an analysis of the nonlinear dynamics of a Charge Pump Phase-Locked Loop. The closed-loop circuit is modelled using equations developed in [1]. A fixed point stability analysis is performed. State space plots, bifurcation diagrams and the presence of a disjoint attractor all indicate a significant level of underlying nonlinear phenomena. Basins of attraction for the system are also examined.

1. Introduction

Phase-lock loops (PLLs) are closed-loop systems with negative feedback. The circuit essentially locks onto the frequency of an incoming signal and maintains this lock by extracting the phase error and aiming to reduce it to zero. The circuit is predominantly used in communications in applications such as frequency synthesis and clock recovery. Recent research has seen significant attempts to better understand the complicated dynamics of PLLs and Digital PLLs through the application of nonlinear theory [2].

The aim of our research is to apply nonlinear dynamical techniques to currently implemented PLLs. In most high frequency applications, a Charge Pump Phase-Locked Loop (CP-PLL) is employed. Modelling of this circuit is complicated by the charge pump action, which essentially makes the circuit time-variant. Two main techniques have been used to model the CP-PLL. The first by Gardner [1] essentially averages the phase error output to give two discrete equations to model the system. The second technique includes the charge-pump action, resulting in a set of decision-based equations [3].

2. CP-PLL Circuit and Modelling

2.1. Basic Circuit Layout

The focus of our research to date has been on the first model [1], which averages the phase error. The CP-PLL consists of four major blocks, Fig. 1.
- The phase-frequency detector, which outputs a pulse proportional to the detected phase error.
- The charge-pump circuit, converting the digital signals U and D into a current, which can have three discrete values: Ip, -Ip and zero.

- The loop filter, converting the charge-pump current into the analog voltage V_{con}. (When combined with Charge-Pump circuit provides integrating zero thus leading to zero static phase error, theoretically)
- The Voltage-Controlled Oscillator (VCO), generating an oscillating signal with a frequency controlled by the voltage V_{con}.

All four of these circuit blocks have non-idealities, which contribute to highly nonlinear behaviour such as frequency spurs, phase jitter and cycle slipping. This has lead to increasing interest in the underlying dynamics of the CP-PLL. This circuit is at the core of developing areas of technology, such as Fractional-N Frequency Synthesis, [4], and high speed clock and data recovery, [5]. Models of Digital PLLs have already exhibited well-documented nonlinear dynamics such as period-doubling bifurcations, limit cycles and restricted basins of attraction [6].
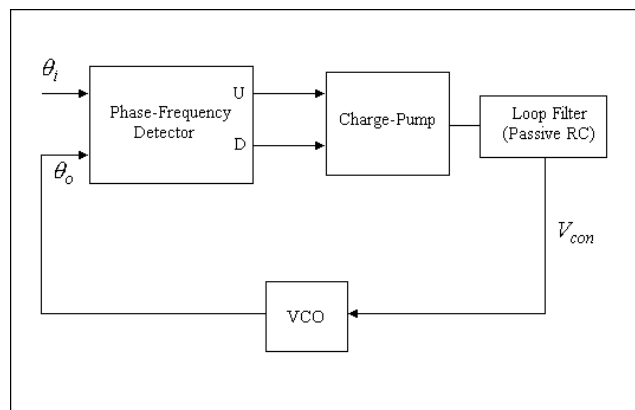

Figure 1: Block Diagram of CP-PLL Circuit

2.2. Model of CP-PLL Circuit

Our research to date has used a model for the CP-PLL from [1]. The model is based on two difference equations, with two state variables. The first state variable is the detected phase error θ_e, the difference between the input phase θ_i and the phase of the output signal of the VCO θ_o. This is an approximation of τ, where τ is equal to the time interval divided by the pulse width of the phase detector output pulses U (positive) and D (negative). In this way the output of the phase detector is represented by only one

variable. U is used to increase the frequency of the VCO output, V_{VCO}, D decreases the frequency of V_{VCO}.

The other state variable is the voltage on the capacitor of the loop filter, V_c. To characterize the charge-pump PLL, four parameters are introduced:

- I_p: the charge pump current
- R and C: the loop filter components
- K_v: the VCO gain, assumed constant

At every period T of the input signal both state variables are calculated. In this way the state variables are updated after a fixed time interval T, resulting in a sampling rate equal to the input frequency. The loop operation is therefore dependent upon the input frequency and the four previously mentioned parameters. The two model equations for the system are (from [7]):

$$\theta_e(k+1) = \theta_e(k) + 2\pi - 2\pi K_v TV_c(k)$$

$$- I_p K_v T\theta_e(k)\left(R + \frac{T}{C} - \frac{|\theta_e(k)|}{2\pi}\frac{T}{2C}\right)\bmod 2\pi \qquad (1)$$

$$V_c(k+1) = V_c(k) + \frac{I_p}{C}\frac{T}{2\pi}\theta_e(k) \qquad (2)$$

3. Nonlinear Analysis of the CP-PLL Model

3.1. Fixed Point Stability of the Model

A fixed point of a map f is a point x^* s. t. $x^* = f(x^*)$. In the case of the PLL, a fixed point corresponds to a locked loop. A non-zero value for θ_e corresponds to a constant or static phase error. The fixed points for the system (1,2) were found to be

$$(\theta_e(k), V_c(k)) = \left(0, \frac{n}{K_v T}\right) \qquad \text{where } n \in Z$$

However, under normal loop conditions, the fixed point of interest is

$$FP(\theta_e(k), V_c(k)) = \left(0, \frac{1}{K_v T}\right)$$

The following substitutions are used for ease of computation:

$$K_1 = K_v T, \; K_2 = I_p RK_v T, \; K_3 = \frac{T}{RC}.$$

Equations (1,2) become

$$\theta_e(k+1) = \theta_e(k) + 2\pi - 2\pi K_1 V_c(k)$$

$$- K_2\theta_e(k)\left(1 + K_3\left(1 - \frac{|\theta_e(k)|}{4\pi}\right)\right)\bmod 2\pi \qquad (3)$$

$$V_c(k+1) = V_c(k) + \frac{K_2 K_3}{2\pi K_1}\theta_e(k) \qquad (4)$$

The Jacobian is therefore

$$Df = \begin{pmatrix} 1 - K_2\left(1 + K_3\left(1 - \frac{|\theta_e(k)|}{4\pi}\right)\right) + \left(\frac{K_2 K_3\theta_e(k)\mathrm{sgn}(\theta_e(k))}{4\pi}\right) & -2\pi K_1 \\ \frac{K_2 K_3}{2\pi K_1} & 1 \end{pmatrix}.$$

Note that even though there is an absolute value term, the partial derivative is valid, as the term is $\alpha|\alpha|$ not $|\alpha|$. Evaluating at the fixed point FP gives (the result is the same for all fixed points)

$$Df = \begin{pmatrix} 1 - K_2(1 + K_3) & -2\pi K_1 \\ \frac{K_2 K_3}{2\pi K_1} & 1 \end{pmatrix}. \qquad (5)$$

$Det(Df - I\lambda) = 0$ gives a characteristic equation of the form

$$\lambda^2 + \lambda(K_2 + K_2 K_3 - 2) + 1 - K_2 = 0. \qquad (6)$$

Which gives eigenvalues equal to

$$\frac{2 - K_2 - K_2 K_3 \pm \sqrt{K_2}\sqrt{K_2 - 4K_3 + 2K_2 K_3 + K_2 K_3^2}}{2}.$$

The condition for stability in a discrete system is that all eigenvalues remain inside the unit circle, this gives a stability limit:

$$C > \frac{I_p K_v T^2}{4 - 2I_p K_v RT}. \qquad (7)$$

3.2. Onset of Period-2 Behaviour

Previous nonlinear analysis of PLLs has revealed the presence of period-doubling bifurcations [2], [6]. The two system equations (3,4) can be used to determine if period-2 behaviour will occur, and the parameter value at which it starts. This is done by using the conditions

$$\theta_e(k+2) = \theta_e(k) \text{ and } V_c(k+2) = V_c(k)$$

and solving:

$$\theta_e(k+2) = \theta_e(k+1) + 2\pi - 2\pi K_1 V_c(k+1)$$

$$- K_2\theta_e(k+1)\left(1 + K_3\left(1 - \frac{|\theta_e(k+1)|}{4\pi}\right)\right)\bmod 2\pi \qquad (8)$$

$$V_c(k+2) = V_c(k+1) + \frac{K_2 K_3}{2\pi K_1}\theta_e(k+1). \qquad (9)$$

Comparing the two equations (8,9) gives the result:

$$4 + K_2 K_3 - 2K_2\left(1 + K_3\left(1 - \frac{|\theta_e(k)|}{4\pi}\right)\right) = 0. \qquad (10)$$

In order to find the onset of period-2 behaviour, the system is assumed, at the onset, to be oscillating very

close about the fixed point. Therefore, assuming $|\theta_e(k)| \approx 0$, and substituting into (10) gives:

$$C = \frac{I_p K_v T^2}{4 - 2I_p K_v RT} \ .$$

This result is the same as that obtained from the fixed point stability analysis, (7). This analysis also provided the result $\theta_e(k+1) = -\theta_e(k)$, confirming the bifurcation to be symmetric about the $\theta_e(k) = 0$ axis.

3.3. Bifurcation Diagram

An interesting aspect of the model equations (1,2) is shown in the bifurcation diagram of Fig. 2(a). Previously PLL models exhibited a period-doubling bifurcation cascade, however with this model this was found not to be the case. In order to get a general view of the bifurcation, the parameter used for the diagram is the normalised natural frequency F_n, defined by $F_n = \frac{T}{2\pi}\sqrt{\frac{K_v I_p}{C}}$. The other parameter is the damping factor, $\zeta = \frac{R}{2}\sqrt{K_v I_p C}$, fixed at 0.4 for the simulations [3].
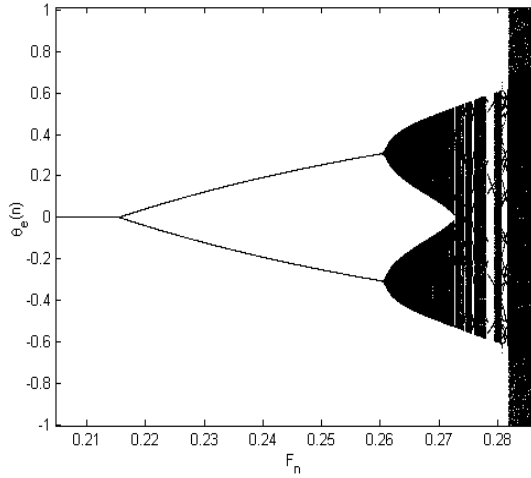

Figure 2(a): Bifurcation Diagram of CP-PLL model

As can be seen in the bifurcation diagram, Fig. 2(a), the system remains at the fixed point, FP, up until a certain value of F_n at which point a pitchfork bifurcation occurs. This point corresponds to the previously calculated onset of period-2 behaviour. Following the period-2 region, another bifurcation results in the emergence of a disjoint attractor. As the normalised natural frequency F_n is increased further, the two parts of the attractor are observed to merge together. This is more clearly shown in the close-up of the bifurcation diagram in Fig. 2(b). This transition can be seen to be interspersed with regions of periodic behaviour. This will be more closely observed in state space in the next section.
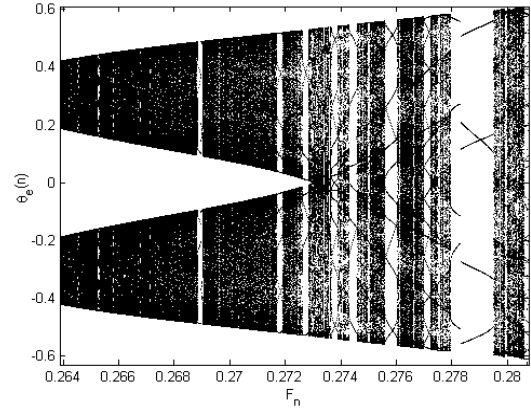

Figure 2(b): Close-up of the Bifurcation Diagram

3.4. Attractor in State Space

The disjoint attractor can be more clearly viewed in state space, Fig. 3(a), which shows the two parts to be roughly elliptical in shape. The state variable V_c is normalised to its fixed point, FP, value. As F_n is increased further, the two parts of the attractor move closer together, Fig. 3(b), and eventually form a single closed loop, as illustrated in Fig. 3(c).
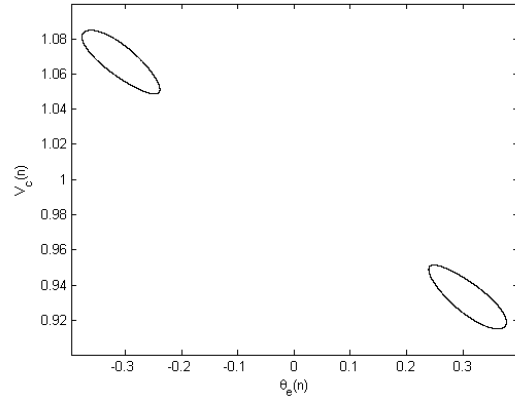

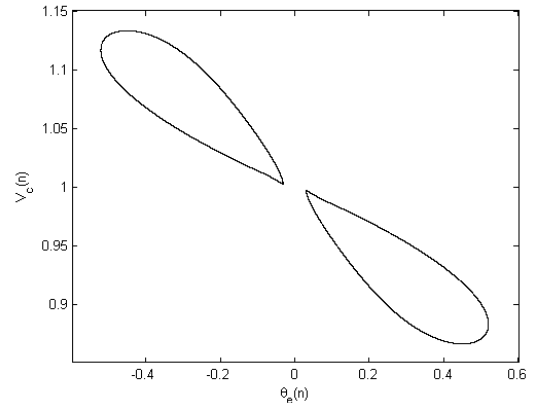*Figure 3(a): State Space of CP-PLL (F_n = 0.262, ζ = 0.4)*

*Figure 3(b): State space of CP-PLL
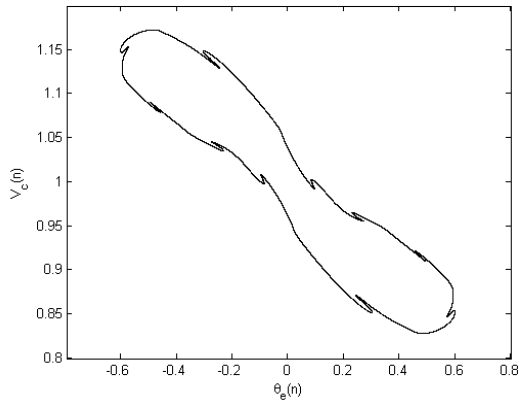(F_n = 0.272, ζ = 0.4)*

Figure 3(c): Resulting single attractor
($F_n = 0.28$, $\zeta = 0.4$)

3.5. Basin of Attraction

The method of nonlinear dynamics used to identify the global behaviour of trajectories is the concept of basins of attraction. The basin of attraction for a particular attractor consists of the set of initial points each of which give rise to a trajectory that approaches the attractor. For the fixed point FP of the CP-PLL the basin of attraction has a fractal structure as shown in Fig. 4, with the largest connected region centred on the fixed point FP.
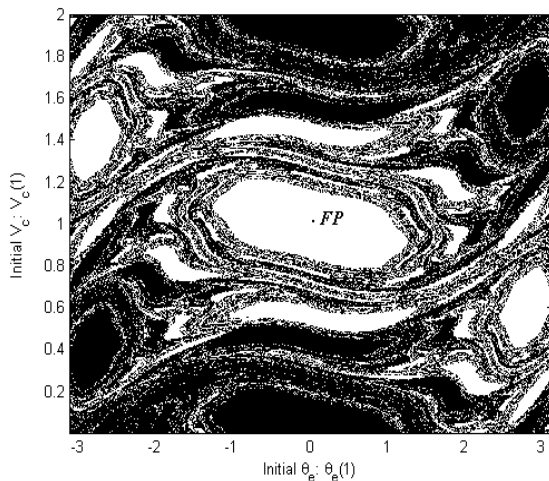

Figure 4: Basin of Attraction (in white) of FP
($Fn = 0.15$, $\zeta = 0.4$)

The central basin shape is found to be roughly elliptical for low values of F_n, becoming increasingly distorted at larger values of F_n. Also, the area of this central region is found to decrease with increasing values of F_n. However, it is also found that increasing the value of the damping factor ζ increases the area of the basin of attraction. The changing area of the central basin is a concern from a design point of view, as most applications would require a full 2π range of initial phase error.

4. Conclusion

The nonlinear dynamics of a model of the Charge-Pump PLL were investigated. A set of fixed points was found. A stability analysis was performed and the boundary found corresponded to the onset of period-2 behaviour. Bifurcation diagrams revealed the presence of a disjoint attractor, and the absence of any further period-doubling bifurcations. The attractor in state space was found to be in two roughly elliptical parts, which merged with increasing F_n to form a single closed loop. Finally, the basin of attraction of the in-lock fixed point FP was found to be fractal in nature. Analysis revealed a significant difference in size and shape of the basin of attraction depending on the choice of design parameters F_n and ζ.

References

[1] F. M. Gardner, "Charge-Pump Phase-Lock Loops," IEEE *Trans. Comm.*, vol. COM-28, No. 11 pp.1849–1858, Nov. 1980.

[2] A. Teplinsky, O. Feely, and A. Rogers, "Phase jitter dynamics of digital phase-locked loops," *IEEE Trans. Circuits Syst. I*, vol. 46, pp. 545-558, May 1999.

[3] M. Van Paemel, "Analysis of a Charge-Pump PLL: A new Model," *IEEE Trans. Commun*, vol. COM-42, No. 7, pp. 2490-2498, July 1994.

[4] M.H. Perrott, M.D. Trott, and C.G. Sodini, "A Modelling Approach for Σ-Δ Fractional-N Frequency Synthesizers Allowing Straightforward Noise Analysis," *IEEE Jour. Solid-State Circuits*, vol. 37, No. 8, pp. 1028-1038, August 2002.

[5] Razavi, B., *Phase-Locking in High-Performance Systems*, IEEE, Wiley, New Jersey, 2003.

[6] G.M. Bernstein, M.A. Lieberman, and A.J. Lichtenberg, "Nonlinear Dynamics of a Digital Phase Locked Loop," *IEEE Trans. Commun*, vol. COM-37, No. 10, pp. 1062-1070, October 1989.

[7] P. Acco, "Why do we linearise Charge Pump PLL equations so early? ," NDES, pp 173-176, June 2001.